UDC 551.554:551.511.6:551.509.313

On the Solution of the Generalized Ekman Equation

JOSEPH T. SCHAEFER—*National Severe Storms Laboratory, NOAA, Norman, Okla.*

ABSTRACT—The generalized Ekman equation is often used for micrometeorological applications. Use of the noniterative numerical technique of superposition reveals that the vertical variation of both the eddy diffusivity and the thermal wind is important to the determination of the wind profile when this equation is applicable.

1. INTRODUCTION

In the planetary boundary layer, the Navier-Stokes equation is often simplified by the assumptions that the flow is steady, horizontal, and homogeneous (Plate 1971). Under these assumptions, the equation can be expressed in complex notation as

$$if[W(z)-G(z)]=\frac{\partial}{\partial z}\left[K(z)\frac{\partial}{\partial z}W(z)\right]. \qquad (1)$$

The symbols are defined as follows:

$i=(-1)^{1/2}$,
f=Coriolis parameter,
$W(z)$=complex horizontal wind, $u+iv$ or (u, v),
u=eastward component of the wind,
v=northward component of the wind,
$G(z)$=complex geostrophic wind,
z=vertical coordinate or height, and
$K(z)$=eddy diffusivity, a real function of z.

If both K and G are defined as constant with height, Ekman's equation results and an analytic solution for the wind field is possible under the boundary conditions

$$W=(0, 0)\equiv 0+0i \qquad \text{at } z=0$$

and

$$\lim_{z\to\infty} W=G.$$

Lettau (1962) assumed that K is a function of height while the geostrophic wind remained constant. Gerrity (1967), in a prognostic boundary-layer model, relaxed the restriction of a constant geostrophic wind with height. But he required that the value of the eddy diffusivity be independent of height. If the vertical distribution of both G and K are known, for at least specific points, a noniterative numerical method of solving eq (1) exists. By using this approach, the inconsistency of assuming a constant eddy momentum transfer coefficient while allowing the eddy conductivity to vary with height in operational boundary-layer models (Hadeen and Friend 1972) can be avoided.

2. METHOD OF SOLUTION

With known distributions of K and G, the generalized Ekman equation is a second-order, linear, complex differential equation; if the wind is specified at the top (z_T) and bottom (z_0) of the boundary layer, numerical integration can be performed based on the principle of superposition. Defining J as a second-order, linear, complex differential operator, we can write eq (1) as

$$J\{W\}=F(z) \qquad (2)$$

with boundary conditions

$$W(z_0)=C_1$$

and

$$W(z_T)=C_2.$$

According to the principle of superposition (Hildebrand 1957), eq (2) can be solved by forming a linear combination of the functions $U(z)$, and $V(z)$, which are nontrivial solutions of

$$J\{U\}=F(z), \qquad U(z_0)=C_1, \qquad U(z_1)=M_1 \qquad (3)$$

and

$$J\{V\}=(0, 0), \qquad V(z_0)=(0, 0), \qquad V(z_1)=M_2. \qquad (4)$$

Here, M_1 and M_2 are arbitrary prescribed complex constants and z_1 is the first gridpoint above the surface. To exclude the trivial solution of eq (4), we cannot define M_2 as zero. The boundary value problems [eq (3) and (4)] can be solved by a marching technique. The solution to eq (2) is the linear combination

$$W(z)=U(z)+AV(z) \qquad (5)$$

where the complex constant, A, is determined by the top boundary condition; that is,

$$A=\frac{C_2-U(z_T)}{V(z_T)}. \qquad (6)$$

If no such constant can be found, no unique solution of eq (2) exists.

In the case of the generalized Ekman equation [eq (1)], the differential operator is

$$J=\left[\frac{\partial}{\partial z}K(z)\frac{\partial}{\partial z}-if\right]$$

and the forcing function is

$$F(z)=-if\,G(z).$$

The prescribed constants can be simply defined as

$$M_1=(0,\,0)$$

and

$$M_2=(1,\,1).$$

This technique is rapid since it is noniterative, and its accuracy is limited only by the finite-difference technique used.

3. EFFECT OF VARIABLE EDDY COEFFICIENT AND THERMAL WIND

To show the utility of the method, we solved eq (1) for four different conditions. The derivatives were approximated to second-order accuracy over a grid spacing of 50 m by means of a "centered" finite-difference scheme. An additional gridpoint was introduced at 2 m in an effort to depict the shelter level. This additional point was handled in the finite-difference mode by generalizing the centered technique to allow for a variable spatial increment.

The first solution (case A) involved the classical Ekman conditions; that is,

$$G=(10,\,0)\text{ m/s},$$

$$f=10^{-4}\text{s}^{-1},$$

$$K=1\ m^2/\text{s},$$

$$W(z_0)=(0,\,0),$$

and

$$W(z_T=1400\text{ m})=G.$$

The results are shown in figure 1A. As the analytic solution demands, v first equals zero at about 444 m, and the cross-isobaric angle [$\tan^{-1}(v/u)$] is 45°.

The second case (case B) allowed the geostrophic wind to back linearly with height so that

$$G(z_0)=(10,\,0),$$

and

$$G(z_T=1400\text{ m})=(8,\,6);$$

the other parameters remain fixed as in A. This hodograph (fig. 1B) is no longer a spiral since the winds at higher levels are forced into close agreement with the backing geostrophic wind. However, little change between this and the classical Ekman case appears in the first 200 m above the surface.

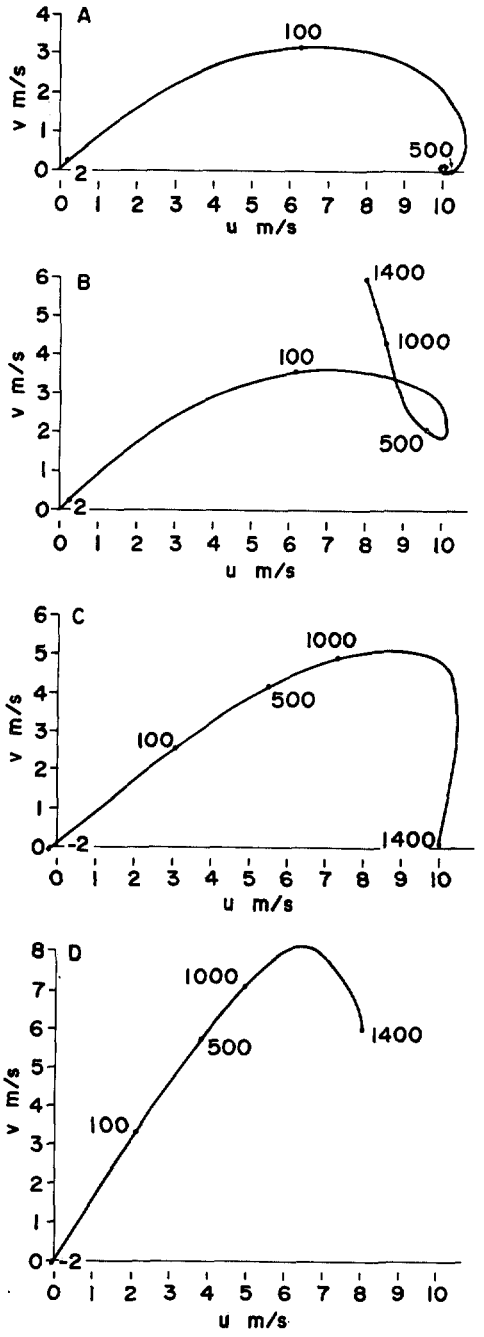

FIGURE 1.—Hodographs for the four cases discussed. Data points are at 50-m increments from surface to 1.4 km with an extra point at 2 m (shelter level).

For case C, the geostrophic wind was held constant (10, 0) and the eddy coefficient was allowed to vary with height in accordance with O'Brien's (1970) profile. Values of K vary from a maximum of 104.5 m²/s at approximately 466 m and asymptotically approach zero at 1400 m. For this profile, the height of the constant flux layer was set at z_1 and $K(z_1)$ was set to 1 m²/s. The other parameters are as in case A. Under these conditions, the wind profile (fig. 1C) exhibits little directional shear with height. Wind speeds in the low levels are much faster than in either of the other cases where the eddy coefficient is held constant with height.

In the final case (case D), both the geostrophic winds and the eddy coefficient are allowed to vary with height.

The baroclinic conditions are the same as in case B while the eddy viscosity is the same as in case C. This example shows the applicability of the solution method. The hodograph (fig. 1D) for this example also demonstrates a nearly constant wind direction with height. However, the thermal wind effect can also be seen by means of the stronger southerly component present in this case as compared to case C.

4. CONCLUSIONS

Even when atmospheric conditions merit application of the generalized Ekman equation (i.e., steady, horizontal, homogeneous flow), the assumption of either constant eddy coefficient or constant geostrophic wind masks the processes occurring and gives fictitious wind profiles. The method of solution superposition is a simple and rapid method of obtaining the wind profile without these restrictive assumptions. Although an eddy coefficient distribution must be assumed, Sasamori (1970) demonstrated that the O'Brien profile is compatible with present knowledge of meteorological turbulence. By using this procedure in presently operational boundary-layer models, the restriction of a constant eddy momentum transfer coefficient could be relaxed.

ACKNOWLEDGMENT

Part of this work was performed while the author was employed by the U.S. Navy Weather Research Facility, Norfolk, Va.

REFERENCES

Gerrity, Joseph P., Jr., "A Physical-Numerical Model for the Prediction of Synoptic-Scale Low Cloudiness," *Monthly Weather Review*, Vol. 95, No. 5, May **1967**, pp 261–282.

Hadeen, Kenneth D., and Friend, Arnold L., "The Air Force Global Weather Center Operational Boundary-Layer Model," *Boundary-Layer Meteorology*, Vol. 3, No. 1, D. Reidel Publishing Co., Dordrecht, Holland, Sept. **1972**, pp. 98–112.

Hildebrand, Francis B., *Introduction to Numerical Analysis*, McGraw-Hill Book Co., Inc., New York, N.Y., **1957**, 511 pp.

Lettau, Heinz H., "Theoretical Wind Spirals in the Boundary Layer of a Barotropic Atmosphere," *Beiträge Zur Physik Der Atmosphäre*, Vol. 35, No. 3/4, Frankfurt, Germany, **1962**, pp. 195–212.

O'Brien, James J., "A Note on the Vertical Structure of the Eddy Exchange Coefficient in the Planetary Boundary Layer," *Journal of the Atmospheric Sciences*, Vol. 27, No. 8, Nov. **1970**, pp. 1213–1215.

Plate, Erich J., *Aerodynamic Characteristics of Atmospheric Boundary Layers*, U.S. Atomic Energy Commission Division of Technical Information Extension, Oak Ridge, Tenn., May **1971**, 190 pp.

Sasamori, Takashi, "A Numerical Study of Atmospheric and Soil Boundary Layers," *Journal of the Atmospheric Sciences*, Vol. 27, No. 8, Nov. **1970**, pp. 1122–1137.

[*Received February 20, 1973*]

UDC 551.521.32:551.508.21:551.507.362.2:551.576(084.1)

PICTURE OF THE MONTH

NOAA 2 Scanning Radiometer Visual and Infrared Imagery Received Real-Time Over a 50,000-Mile Transmission Link

HENRY W. BRANDLI, JOHN W. OLIVER, and RAMON J. ESTU—*Detachment 11, 6th Weather Wing, Air Weather Service, Patrick Air Force Base, Fla.*

ITOS D (NOAA 2) was launched on Oct. 15, 1972. Its simultaneous scanning radiometer imagery of video and infrared is a new system designed to transmit imagery below the satellite night and day. The Detachment 11 forecast facility at Cape Kennedy, Fla., was the first operational site in the world to receive and process this highest quality, real-time, expanded, simultaneous scanning radiometer data. Detachment 11 uses a modified

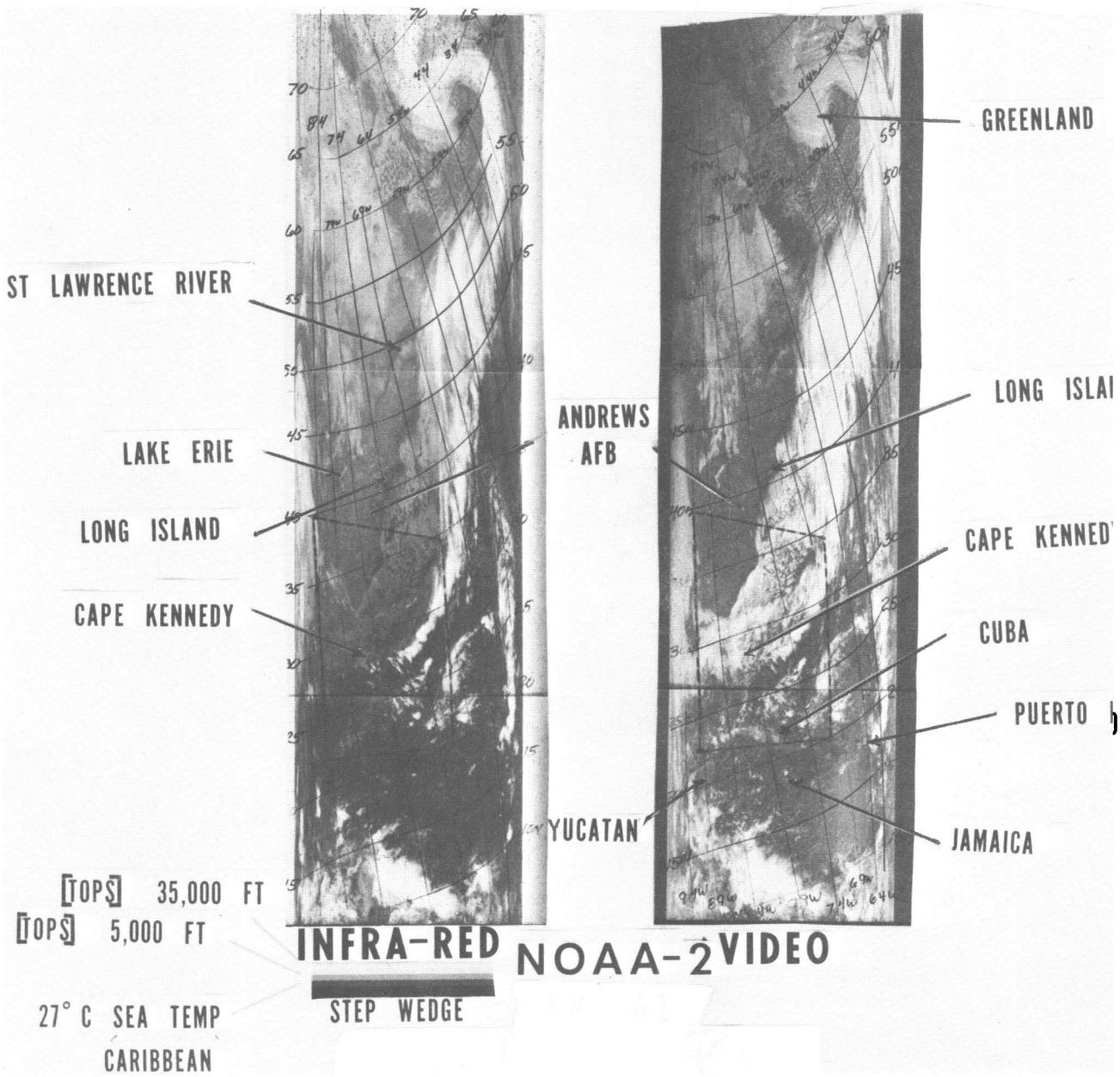

FIGURE 1.—Geographically gridded simultaneous NOAA 2 scanning radiometry imagery for 1400–1423 GMT, Oct. 20, 1972.

Muirhead 115B/1 with a Leonessa module 141,[1] similar to the system of the Air Force Cambridge Research Laboratories. Figure 1 is an example of the simultaneous scanning radiometer (SR) imagery, which is received in real time, gridded geographically, and interpreted meteorologically by Air Weather Service forecasters at Cape Kennedy. The photographs in figure 1 have been reduced; the actual width of the imagery is $5\frac{3}{32}$ in.

An example of a quick local area analysis that can be derived exclusively from the satellite data is shown in figure 2. This analysis used *only* the visual and infrared intelligence contained within the quadrilateral outlined around Cape Kennedy in figure 1. Densitometer calibrations are used to change the infrared radiance imagery to temperatures and thus deduce the cloud tops (Myers et al. 1970). Quantitative measurements are difficult due to the many variables involved; however, due to the window (10.5–12.5μm) used in the scanning radiometer sensor, sufficient accuracy is obtained to allow adequate determination of cloud types and their approximate levels.

[1] Mention of a commercial product does not constitute an endorsement.

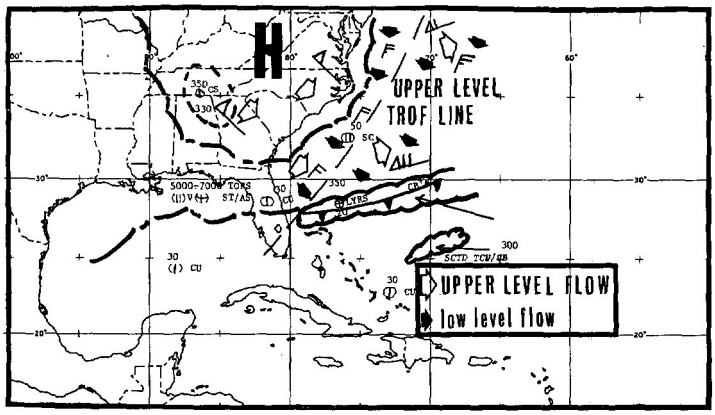

FIGURE 2.—Analysis derived from the visual and IR quadrilateral on figure 1 for 1415 GMT, Oct. 20, 1972.

An excellent example of operational use of this data and technique occurred during the APOLLO 17 mission on Dec. 6, 1972. Figure 3 is a sample of the simultaneous video and infrared data received in real time at Cape Kennedy from Ascension Island—approximately a 50,000 n.mi. transmission hookup via the COMSAT Communications Satellite. This critical imagery was used to provide the Apollo Range Instrumented Aircraft (ARIA) with real-time decision-making assistance for staging bases on the west coast of Africa as well as the crucial positioning of the aircraft during the translunar injection (TLI) phase of the mission. The extent of the stratus clouds in the vicinity of Roberts Field, Monrovia, Liberia, is clearly depicted using the visual and infrared data together. In addition, the location of the subtropical jet is easily inferred from the SR data and was all important in the westward shift of the TLI as the launch of APOLLO 17 was delayed. Confirmation of the jet stream speed was obtained from ARIA aircraft operating in the area.

In addition, the APOLLO 17 astronauts were briefed on the weather at the launch area and the Atlantic abort area using the Detachment 11 high-quality, simultaneous SR data prior to liftoff.

REFERENCE

Myers, Robert F., Sprague, Edward D., and Mareiro, Barry A., "Controlled Processing of Direct Readout Data From Weather Satellites," *Final Report* No. AFCRL-70-0589, U.S. Air Force Research Laboratories, Hanscom Field, Mass., Oct. 1970, 66 pp

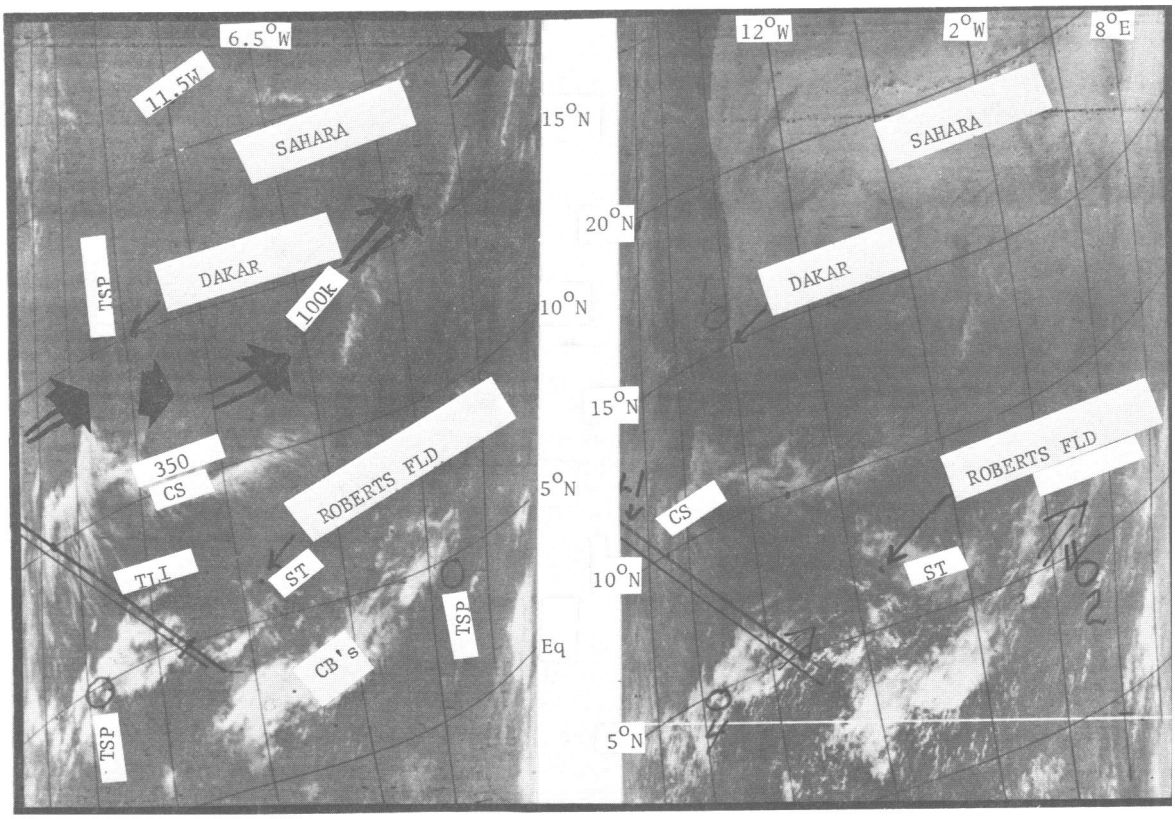

FIGURE 3.—Real-time simultaneous video and infrared from Ascension Island to Cape Kennedy, a transmission over more than 50,000 n.mi.